US011721296B2

(12) **United States Patent**
Crounse

(10) **Patent No.: US 11,721,296 B2**
(45) **Date of Patent: Aug. 8, 2023**

(54) **METHOD AND APPARATUS FOR RENDERING COLOR IMAGES**

(71) Applicant: **E Ink Corporation**, Billerica, MA (US)

(72) Inventor: **Kenneth R. Crounse**, Somerville, MA (US)

(73) Assignee: **E Ink Corporation**, Billerica, MA (US)

(*) Notice: Subject to any disclaimer, the term of this patent is extended or adjusted under 35 U.S.C. 154(b) by 19 days.

(21) Appl. No.: **17/516,795**

(22) Filed: **Nov. 2, 2021**

(65) **Prior Publication Data**

US 2022/0139341 A1 May 5, 2022

Related U.S. Application Data

(60) Provisional application No. 63/108,855, filed on Nov. 2, 2020.

(51) **Int. Cl.**
G09G 3/34 (2006.01)
G09G 3/38 (2006.01)

(52) **U.S. Cl.**
CPC ***G09G 3/344*** (2013.01); ***G09G 3/38*** (2013.01); *G09G 2320/0666* (2013.01); *G09G 2340/06* (2013.01)

(58) **Field of Classification Search**
CPC .. G09G 3/344; G09G 3/38; G09G 2320/0666; G09G 2340/06; G09G 3/2044; G09G 5/02
See application file for complete search history.

(56) **References Cited**

U.S. PATENT DOCUMENTS

5,930,026	A	7/1999	Jacobson
6,017,584	A	1/2000	Albert et al.
6,445,489	B1	9/2002	Jacobson et al.
6,504,524	B1	1/2003	Gates et al.
6,512,354	B2	1/2003	Jacobson et al.
6,531,997	B1	3/2003	Gates et al.
6,545,797	B2	4/2003	Chen et al.
6,664,944	B1	12/2003	Albert et al.
6,753,999	B2	6/2004	Zehner et al.
6,788,452	B2	9/2004	Liang et al.
6,825,970	B2	11/2004	Goenaga et al.
6,900,851	B2	5/2005	Morrison et al.
6,995,550	B2	2/2006	Jacobson et al.
7,012,600	B2	3/2006	Zehner et al.
7,023,420	B2	4/2006	Comiskey et al.
7,034,783	B2	4/2006	Gates et al.
7,038,656	B2	5/2006	Liang et al.

(Continued)

OTHER PUBLICATIONS

Korean Intellectual Property Office, "International Search Report and Written Opinion", PCT/US2021/057648, dated Feb. 16, 2022.

(Continued)

Primary Examiner — Mark W Regn
(74) *Attorney, Agent, or Firm* — Brian D. Bean

(57) **ABSTRACT**

There are provided methods for driving an electro-optic display A method for driving an electro-optic display having a plurality of display pixels, the method comprises receiving an input image, processing the input image to create color separation cumulate, and using a threshold array to process the color separation cumulate to generate colors for the electro-optic display.

13 Claims, 10 Drawing Sheets
(8 of 10 Drawing Sheet(s) Filed in Color)

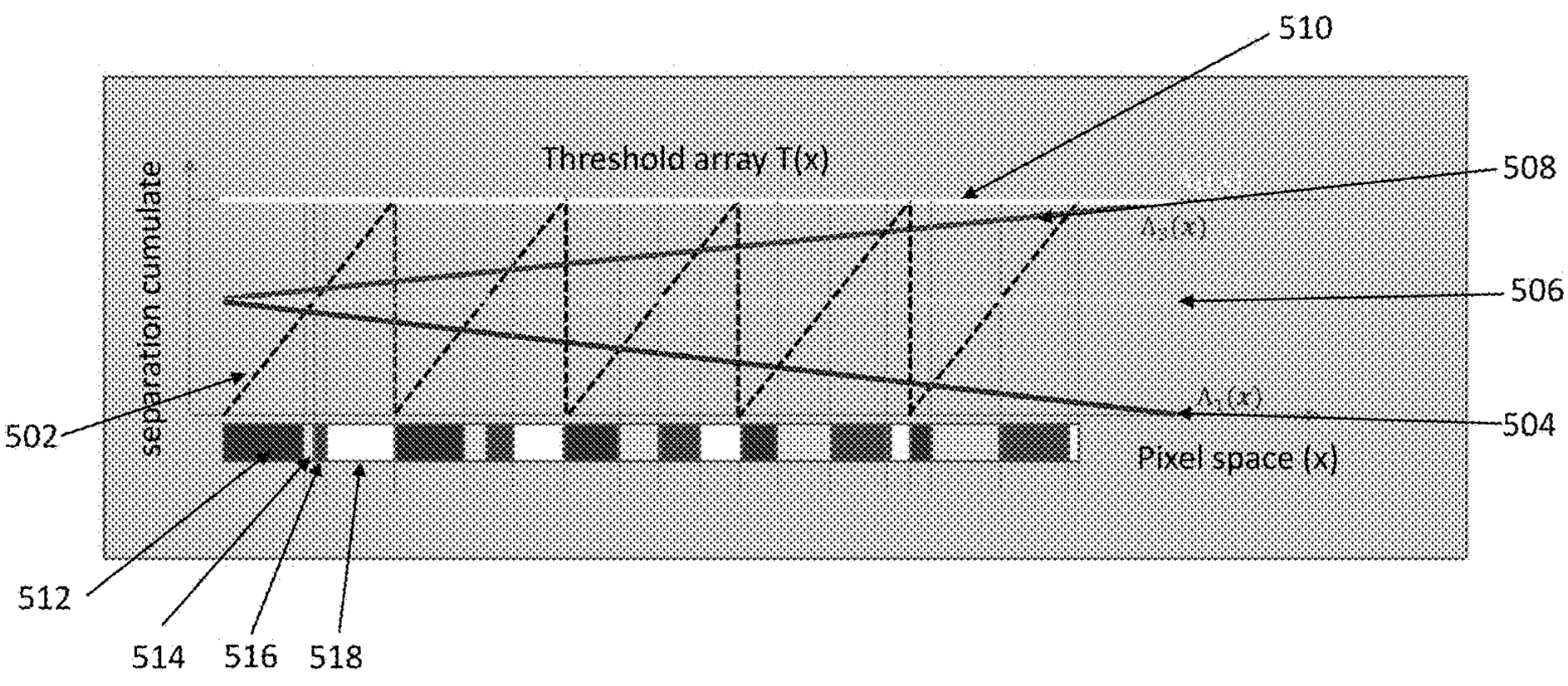

(56) **References Cited**

U.S. PATENT DOCUMENTS

7,038,670	B2	5/2006	Liang et al.
7,046,228	B2	5/2006	Liang et al.
7,052,571	B2	5/2006	Wang et al.
7,054,038	B1	5/2006	Ostromoukhov et al.
7,061,166	B2	6/2006	Kuniyasu
7,061,662	B2	6/2006	Chung et al.
7,075,502	B1	7/2006	Drzaic et al.
7,116,466	B2	10/2006	Whitesides et al.
7,119,772	B2	10/2006	Amundson et al.
7,167,155	B1	1/2007	Albert et al.
7,177,066	B2	2/2007	Chung et al.
7,193,625	B2	3/2007	Danner et al.
7,202,847	B2	4/2007	Gates
7,259,744	B2	8/2007	Arango et al.
7,327,511	B2	2/2008	Whitesides et al.
7,385,751	B2	6/2008	Chen et al.
7,408,699	B2	8/2008	Wang et al.
7,453,445	B2	11/2008	Amundson
7,492,339	B2	2/2009	Amundson
7,492,505	B2	2/2009	Liang et al.
7,528,822	B2	5/2009	Amundson et al.
7,583,251	B2	9/2009	Arango et al.
7,602,374	B2	10/2009	Zehner et al.
7,612,760	B2	11/2009	Kawai
7,667,684	B2	2/2010	Jacobson et al.
7,679,599	B2	3/2010	Kawai
7,683,606	B2	3/2010	Kang et al.
7,729,039	B2	6/2010	LeCain et al.
7,787,169	B2	8/2010	Abramson et al.
7,800,813	B2	9/2010	Wu et al.
7,839,564	B2	11/2010	Whitesides et al.
7,859,742	B1	12/2010	Chiu et al.
7,910,175	B2	3/2011	Webber
7,952,557	B2	5/2011	Amundson
7,952,790	B2	5/2011	Honeyman et al.
7,982,479	B2	7/2011	Wang et al.
7,982,941	B2	7/2011	Lin et al.
7,999,787	B2	8/2011	Amundson et al.
8,040,594	B2	10/2011	Paolini, Jr. et al.
8,054,526	B2	11/2011	Bouchard
8,077,141	B2	12/2011	Duthaler et al.
8,098,418	B2	1/2012	Paolini, Jr. et al.
8,125,501	B2	2/2012	Amundson et al.
8,139,050	B2	3/2012	Jacobson et al.
8,159,636	B2	4/2012	Sun et al.
8,174,490	B2	5/2012	Whitesides et al.
8,243,013	B1	8/2012	Sprague et al.
8,274,472	B1	9/2012	Wang et al.
8,289,250	B2	10/2012	Zehner et al.
8,300,006	B2	10/2012	Zhou et al.
8,314,784	B2	11/2012	Ohkami et al.
8,363,299	B2	1/2013	Paolini, Jr. et al.
8,373,649	B2	2/2013	Low et al.
8,384,658	B2	2/2013	Albert et al.
8,422,116	B2	4/2013	Sprague et al.
8,456,414	B2	6/2013	Lin et al.
8,462,102	B2	6/2013	Wong et al.
8,503,063	B2	8/2013	Sprague
8,514,168	B2	8/2013	Chung et al.
8,537,105	B2	9/2013	Chiu et al.
8,558,783	B2	10/2013	Wilcox et al.
8,558,786	B2	10/2013	Lin
8,558,855	B2	10/2013	Sprague et al.
8,576,164	B2	11/2013	Sprague et al.
8,576,259	B2	11/2013	Lin et al.
8,576,470	B2	11/2013	Paolini, Jr. et al.
8,576,475	B2	11/2013	Huang et al.
8,605,032	B2	12/2013	Liu et al.
8,605,354	B2	12/2013	Zhang et al.
8,649,084	B2	2/2014	Wang et al.
8,665,206	B2	3/2014	Lin et al.
8,670,174	B2	3/2014	Sprague et al.
8,681,191	B2	3/2014	Yang et al.
8,704,756	B2	4/2014	Lin
8,717,664	B2	5/2014	Wang et al.
8,750,390	B2	6/2014	Sun et al.
8,786,935	B2	7/2014	Sprague
8,797,634	B2	8/2014	Paolini, Jr. et al.
8,810,525	B2	8/2014	Sprague
8,873,129	B2	10/2014	Paolini, Jr. et al.
8,902,153	B2	12/2014	Bouchard et al.
8,902,491	B2	12/2014	Wang et al.
8,917,439	B2	12/2014	Wang et al.
8,928,562	B2	1/2015	Gates et al.
8,928,641	B2	1/2015	Chiu et al.
8,941,885	B2	1/2015	Nishikawa et al.
8,964,282	B2	2/2015	Wang et al.
8,976,444	B2	3/2015	Zhang et al.
9,013,394	B2	4/2015	Lin
9,013,783	B2	4/2015	Sprague
9,019,197	B2	4/2015	Lin
9,019,198	B2	4/2015	Lin et al.
9,019,318	B2	4/2015	Sprague et al.
9,082,352	B2	7/2015	Cheng et al.
9,116,412	B2	8/2015	Lin
9,146,439	B2	9/2015	Zhang
9,171,508	B2	10/2015	Sprague et al.
9,182,646	B2	11/2015	Paolini, Jr. et al.
9,195,111	B2	11/2015	Anseth et al.
9,199,441	B2	12/2015	Danner
9,218,773	B2	12/2015	Sun et al.
9,224,338	B2	12/2015	Chan et al.
9,224,342	B2	12/2015	Sprague et al.
9,224,344	B2	12/2015	Chung et al.
9,230,492	B2	1/2016	Harrington et al.
9,251,736	B2	2/2016	Lin et al.
9,262,973	B2	2/2016	Wu et al.
9,285,649	B2	3/2016	Du et al.
9,299,294	B2	3/2016	Lin et al.
9,341,916	B2	5/2016	Telfer et al.
9,360,733	B2	6/2016	Wang et al.
9,361,836	B1	6/2016	Telfer et al.
9,390,066	B2	7/2016	Smith et al.
9,390,661	B2	7/2016	Chiu et al.
9,423,666	B2	8/2016	Wang et al.
9,459,510	B2	10/2016	Lin
9,460,666	B2	10/2016	Sprague et al.
9,495,918	B2	11/2016	Harrington et al.
9,501,981	B2	11/2016	Lin et al.
9,513,527	B2	12/2016	Chan et al.
9,513,743	B2	12/2016	Sjodin et al.
9,514,667	B2	12/2016	Lin
9,541,814	B2	1/2017	Lin et al.
9,612,502	B2	4/2017	Danner et al.
9,613,587	B2	4/2017	Halfman et al.
9,620,048	B2	4/2017	Sim et al.
9,671,668	B2	6/2017	Chan et al.
9,672,766	B2	6/2017	Sjodin
9,691,333	B2	6/2017	Cheng et al.
9,721,495	B2	8/2017	Harrington et al.
9,759,980	B2	9/2017	Du et al.
9,792,861	B2	10/2017	Chang et al.
9,792,862	B2	10/2017	Hung et al.
9,812,073	B2	11/2017	Lin et al.
10,027,963	B2	7/2018	Su et al.
10,162,242	B2	12/2018	Wang et al.
10,209,556	B2	2/2019	Rosenfeld et al.
10,229,641	B2	3/2019	Yang et al.
10,319,313	B2	6/2019	Harris et al.
10,339,876	B2	7/2019	Lin et al.
10,467,984	B2	11/2019	Buckley et al.
10,672,350	B2	6/2020	Amundson et al.
11,151,951	B2	10/2021	Lin et al.
2003/0102858	A1	6/2003	Jacobson et al.
2004/0246562	A1	12/2004	Chung et al.
2005/0253777	A1	11/2005	Zehner et al.
2007/0103427	A1	5/2007	Zhou et al.
2007/0176912	A1	8/2007	Beames et al.
2008/0024429	A1	1/2008	Zehner
2008/0024482	A1	1/2008	Gates et al.
2008/0043318	A1	2/2008	Whitesides et al.
2008/0136774	A1	6/2008	Harris et al.
2008/0303780	A1	12/2008	Sprague et al.
2009/0225398	A1	9/2009	Duthaler et al.

(56) **References Cited**

U.S. PATENT DOCUMENTS

2010/0156780	A1	6/2010	Jacobson et al.	
2010/0194733	A1	8/2010	Lin et al.	
2010/0194789	A1	8/2010	Lin et al.	
2010/0220121	A1	9/2010	Zehner et al.	
2010/0265561	A1	10/2010	Gates et al.	
2011/0043543	A1	2/2011	Chen et al.	
2011/0063314	A1	3/2011	Chiu et al.	
2011/0175875	A1	7/2011	Lin et al.	
2011/0221740	A1	9/2011	Yang et al.	
2012/0001957	A1	1/2012	Liu et al.	
2012/0098740	A1	4/2012	Chiu et al.	
2013/0046803	A1	2/2013	Parmar et al.	
2013/0063333	A1	3/2013	Arango et al.	
2013/0249782	A1	9/2013	Wu et al.	
2014/0055840	A1	2/2014	Zang et al.	
2014/0078576	A1	3/2014	Sprague	
2014/0204012	A1	7/2014	Wu et al.	
2014/0240210	A1	8/2014	Wu et al.	
2014/0253425	A1	9/2014	Zalesky et al.	
2014/0293398	A1	10/2014	Wang et al.	
2014/0362213	A1	12/2014	Tseng	
2015/0262255	A1	9/2015	Khajehnouri et al.	
2015/0268531	A1	9/2015	Wang et al.	
2015/0301246	A1	10/2015	Zang et al.	
2016/0180777	A1	6/2016	Lin et al.	
2019/0080666	A1 *	3/2019	Chappalli	G09G 3/006

OTHER PUBLICATIONS

Pappas, Thrasyvoulos N. "Model-based halftoning of color images." IEEE Transactions on image processing 6.7 (1997): 1014-24.

Ostromoukhov, Victor et al., "Multi-Color and Artistic Dithering", Proceedings of the 26th Annual Conference on Computer Graphics and Interactive Techniques, ACM Press / Addison-Wesley Publishing Co. (1999).

Ulichney, Robert A., "Void-and-Cluster Method for Dither Array Generation", Human Vision Visual Processing and Digital Display IV, vol. 1913, International Society for Optics and Photonics, (1993).

* cited by examiner

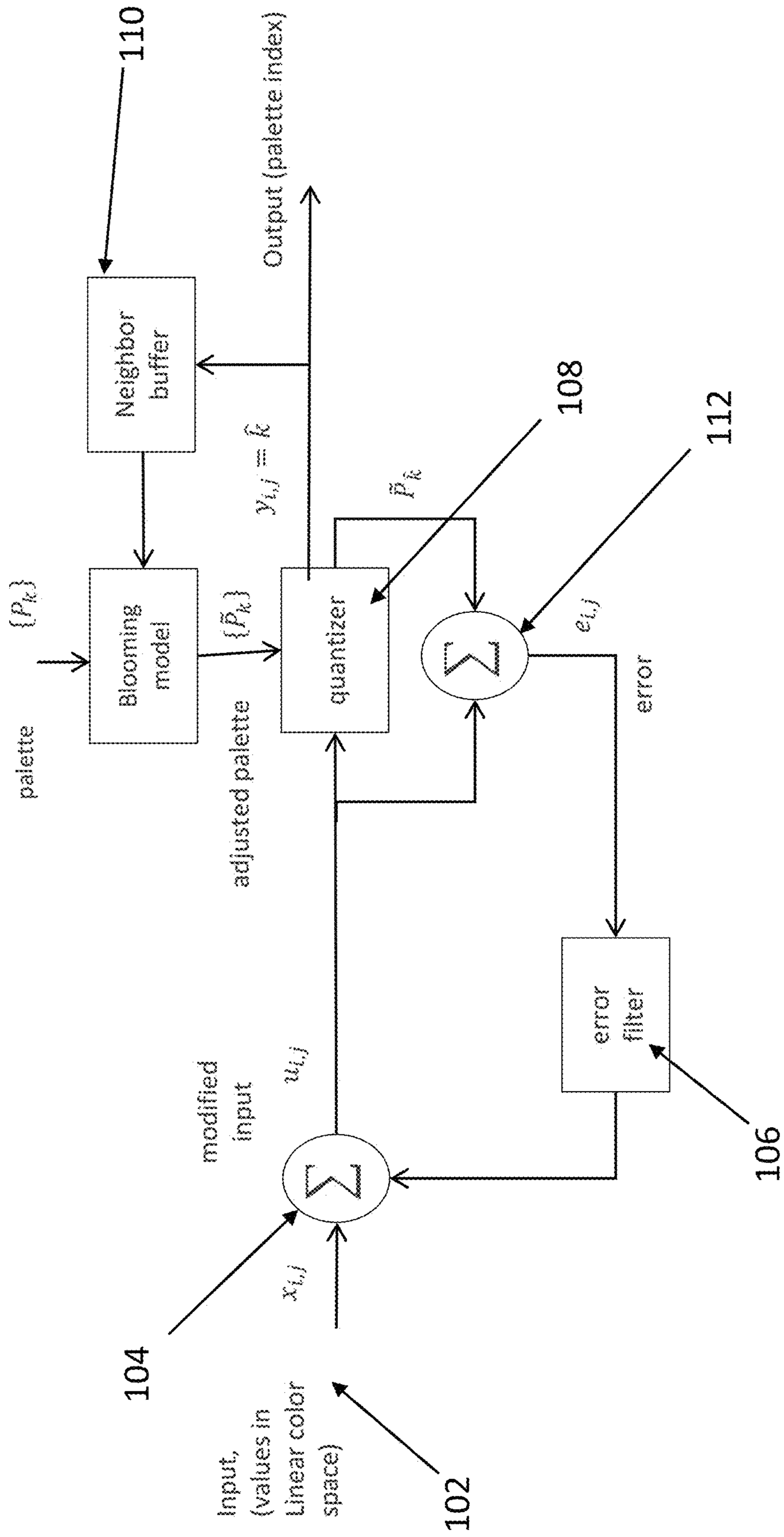
110
Output (palette index)
Neighbor buffer
$y_{i,j} = \hat{k}$
108
112
$\tilde{P}_k$
$\{P_k\}$
Blooming model
$\{\tilde{P}_k\}$
quantizer
$e_{i,j}$
palette
adjusted palette
error
error filter
modified input
$u_{i,j}$
$x_{i,j}$
104
Input, (values in Linear color space)
102
106

Figure 1

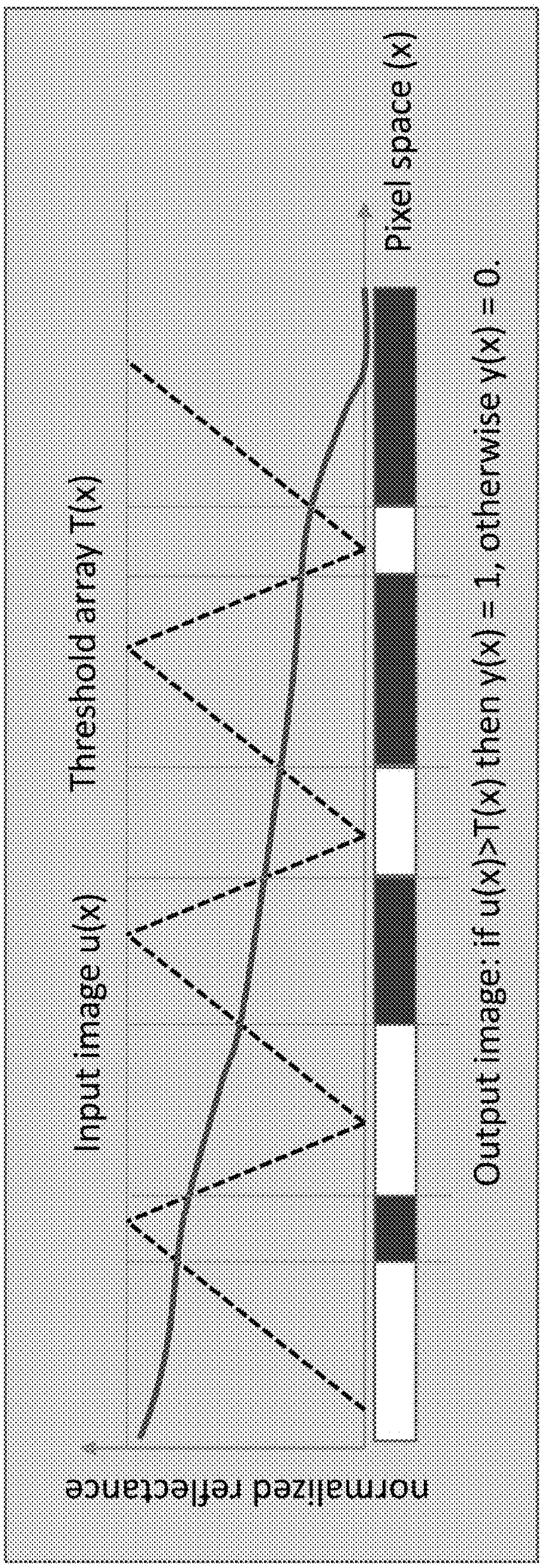
Pixel space (x)
Threshold array T(x)
Input image u(x)
Output image: if u(x)>T(x) then y(x) = 1, otherwise y(x) = 0.
normalized reflectance

Figure 2

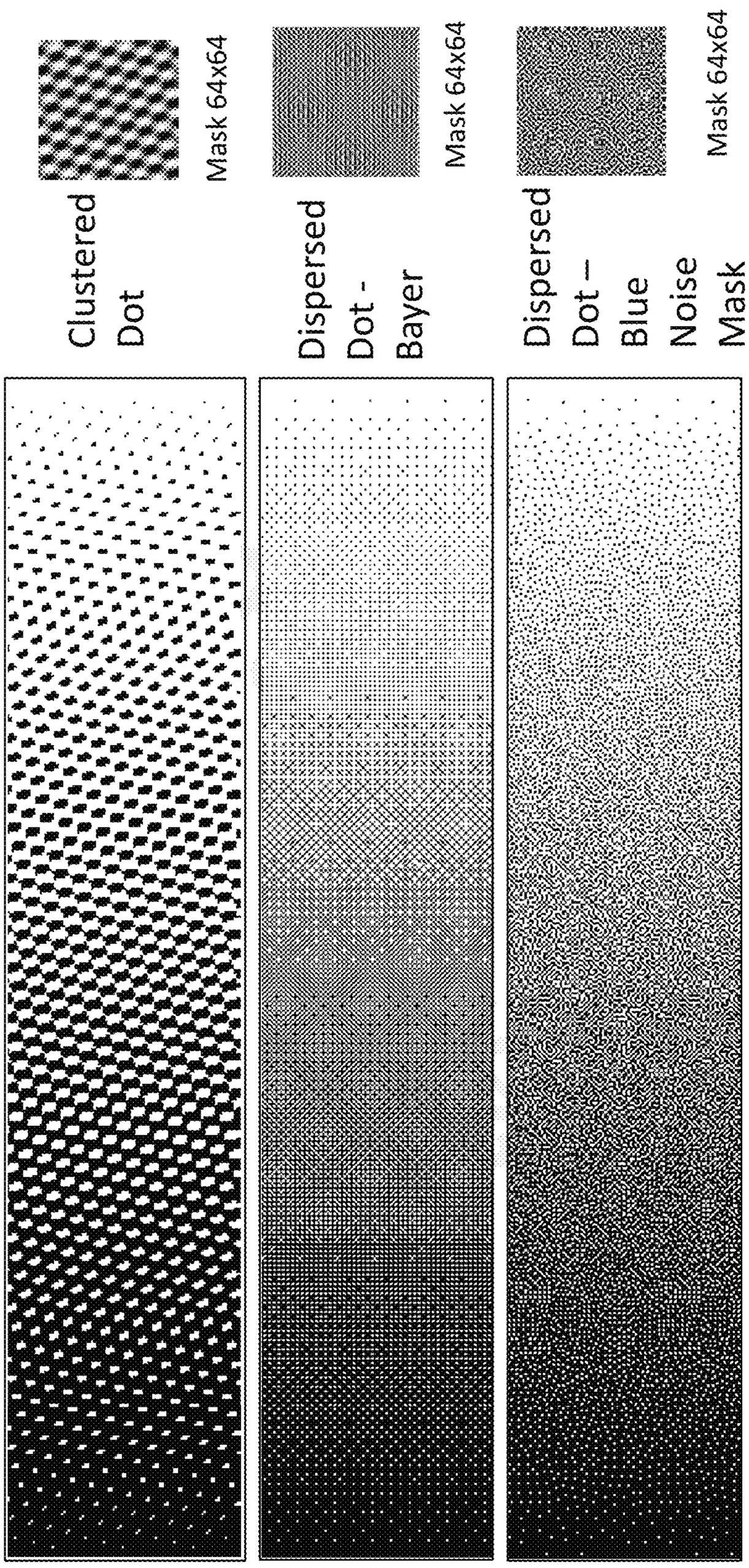
Clustered Dot
Mask 64x64
Dispersed Dot - Bayer
Mask 64x64
Dispersed Dot – Blue Noise Mask
Mask 64x64

Figure 3

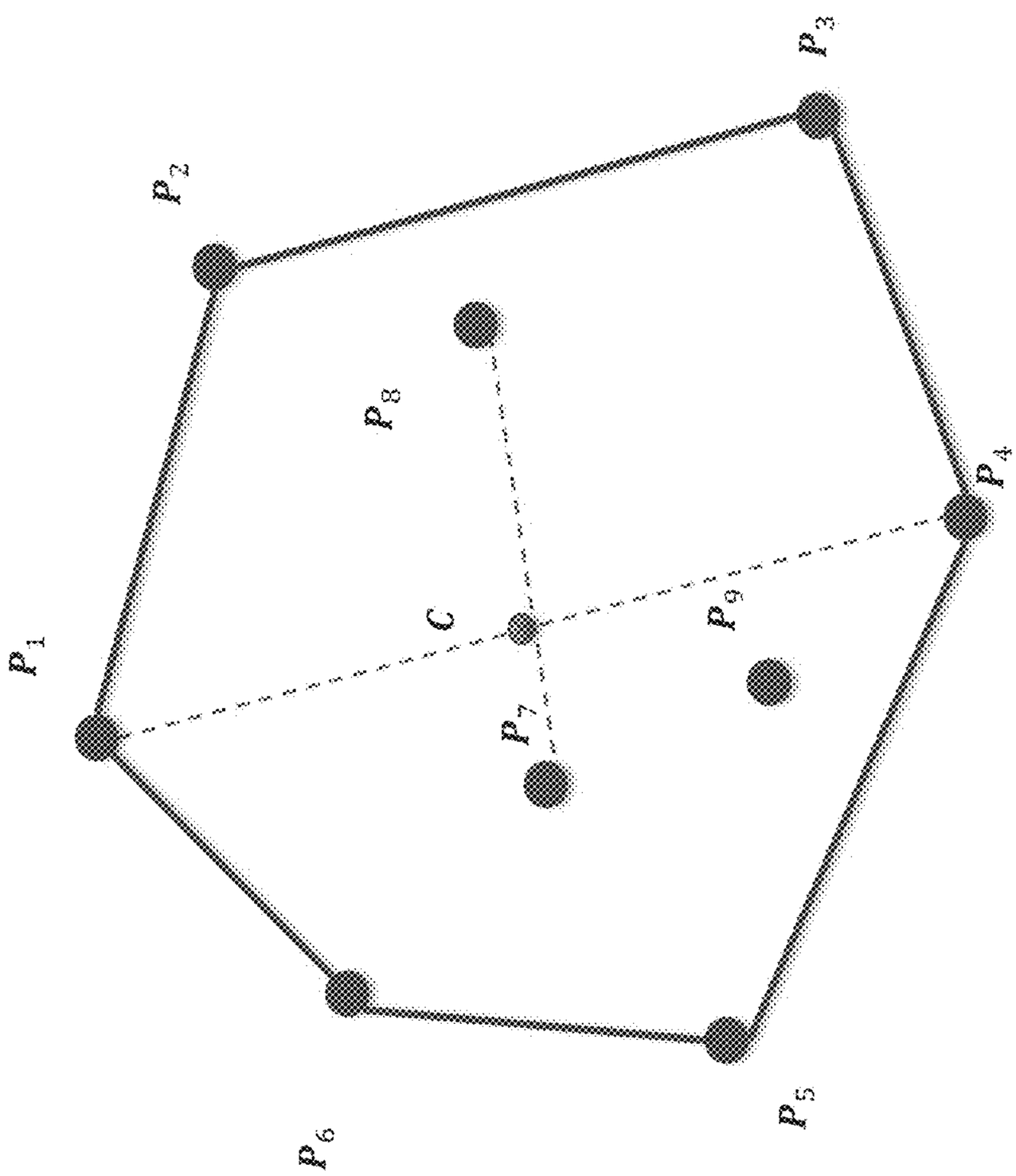

Figure 4

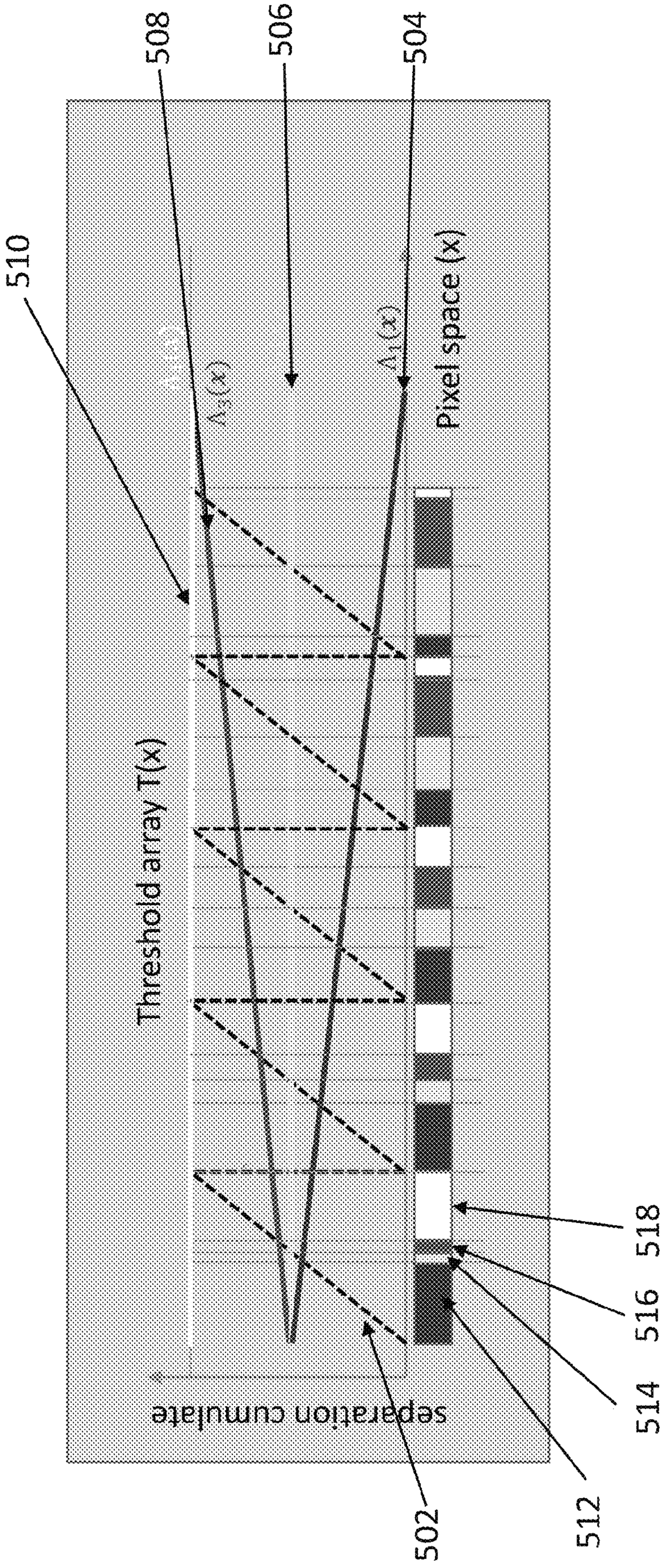
508
506
504
510
$\Lambda_2(x)$
$\Lambda_1(x)$
Pixel space (x)
Threshold array T(x)
separation cumulate
502
512
514
516
518

Figure 5

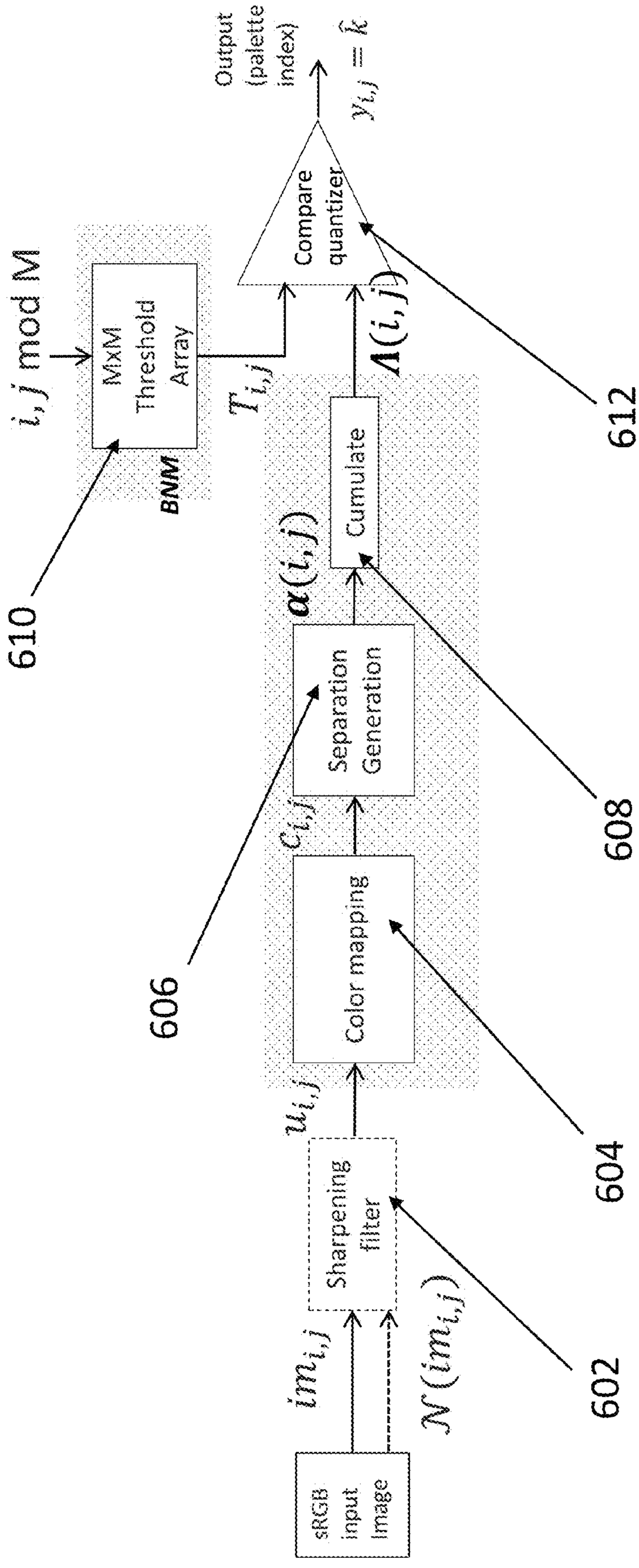
Output (palette index)
$y_{i,j} = \hat{k}$
Compare quantizer
$T_{i,j}$
MxM Threshold Array
BNM
$i, j \bmod M$
610
$A(i,j)$
612
$\alpha(i,j)$
Cumulate
608
$c_{i,j}$
Separation Generation
606
$u_{i,j}$
Color mapping
604
$im_{i,j}$
Sharpening filter
$\mathcal{N}(im_{i,j})$
602
sRGB input Image

Figure 6

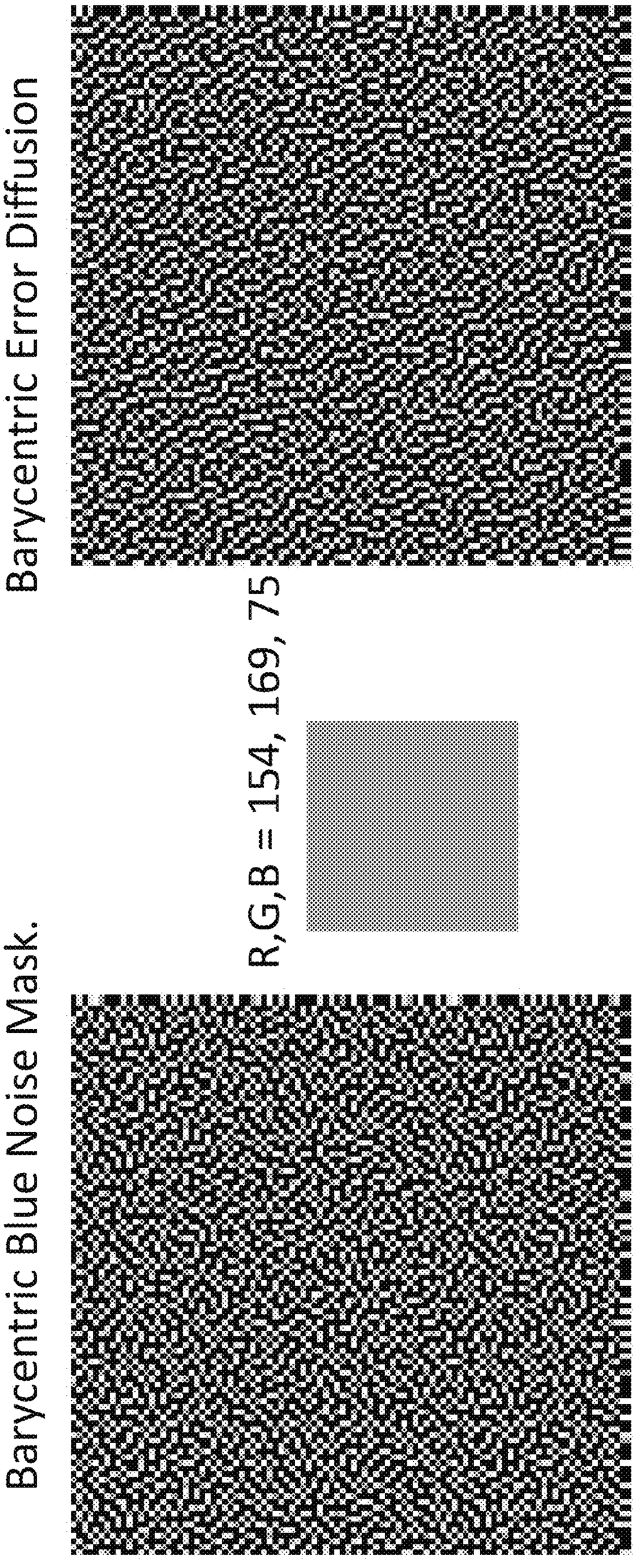
Source spectrum dithering using Kuhn decomposition
Figure 7
R,G,B = 154, 169, 75
Barycentric Blue Noise Mask.
Barycentric Error Diffusion

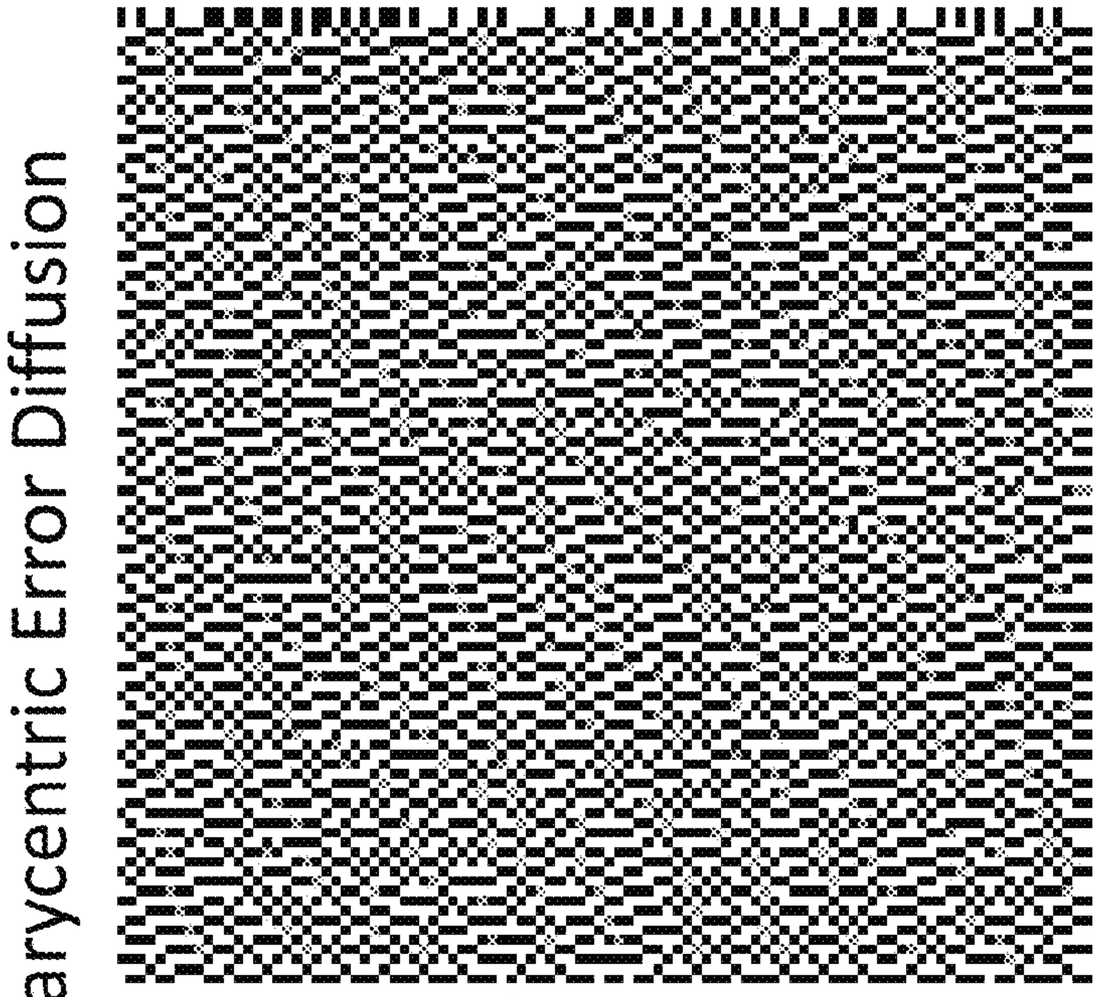

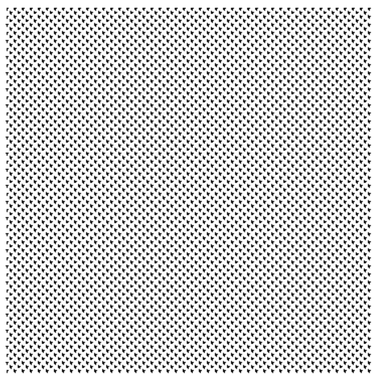

R,G,B = 195, 201, 196

Figure 8

Source space dithering using Kuhn decomposition

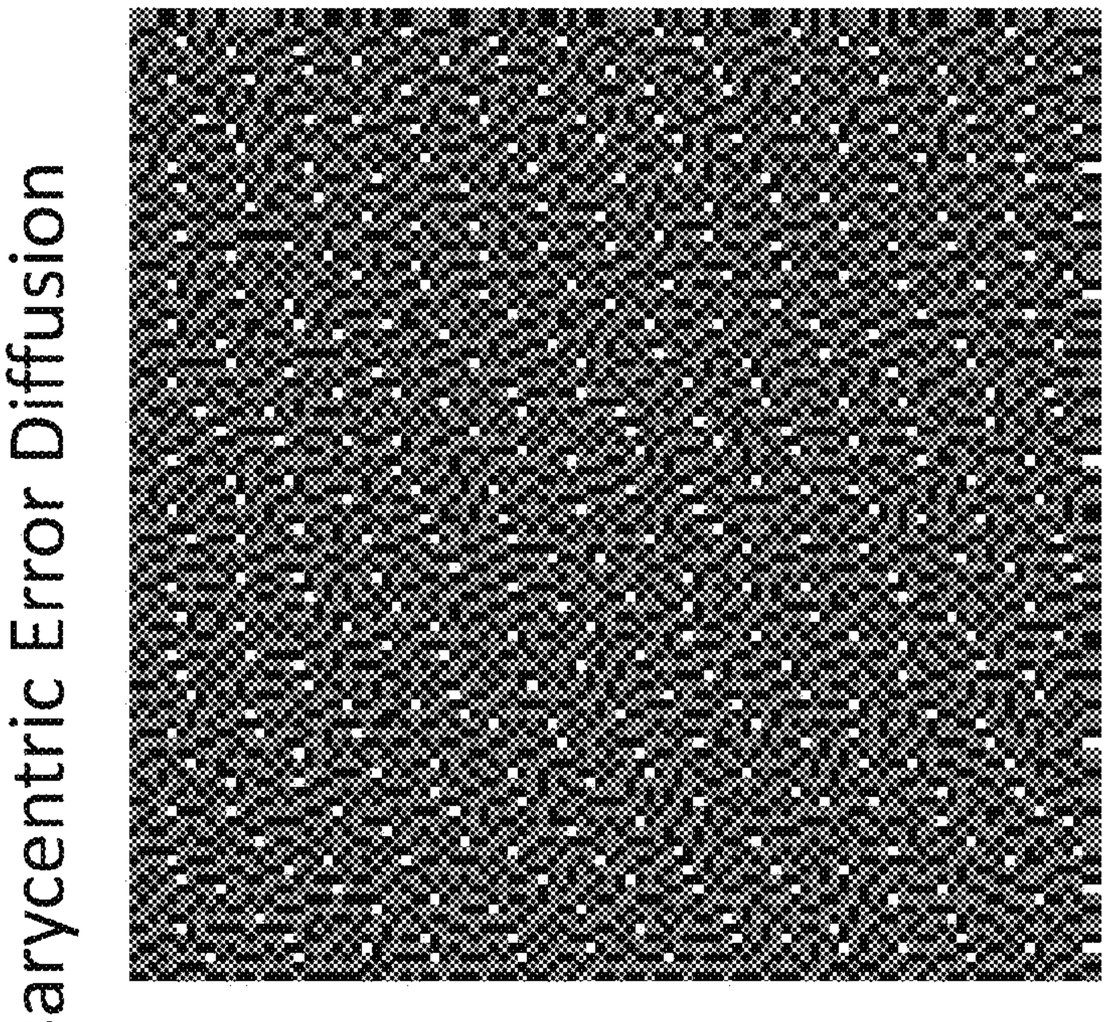

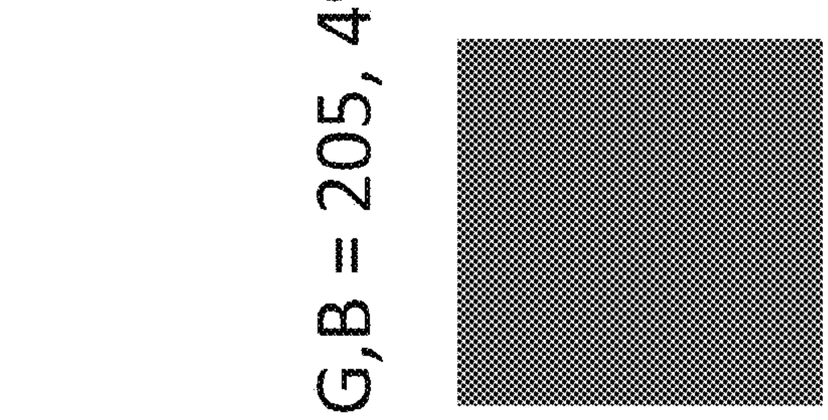

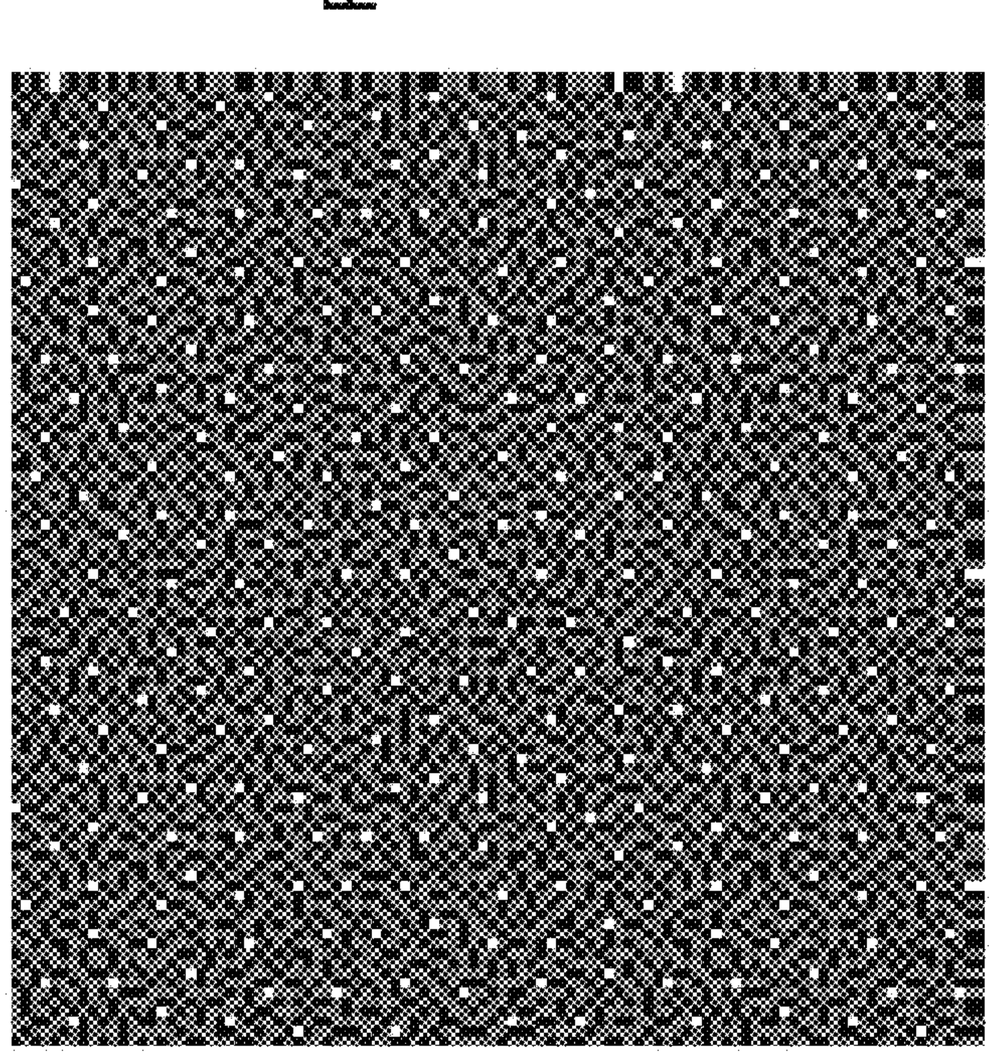

Figure 9

Source space dithering using Kuhn decomposition

Source space dithering using Kuhn decomposition

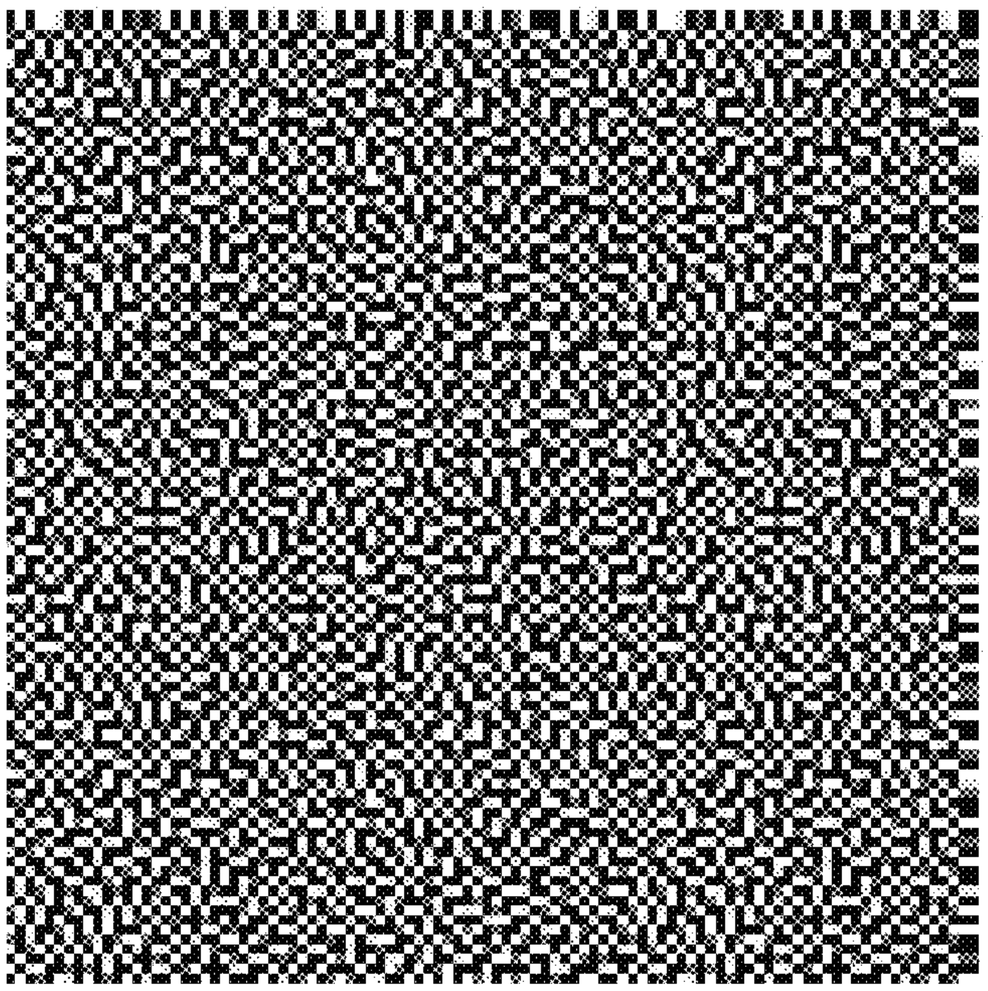

Barycentric Blue Noise Mask.

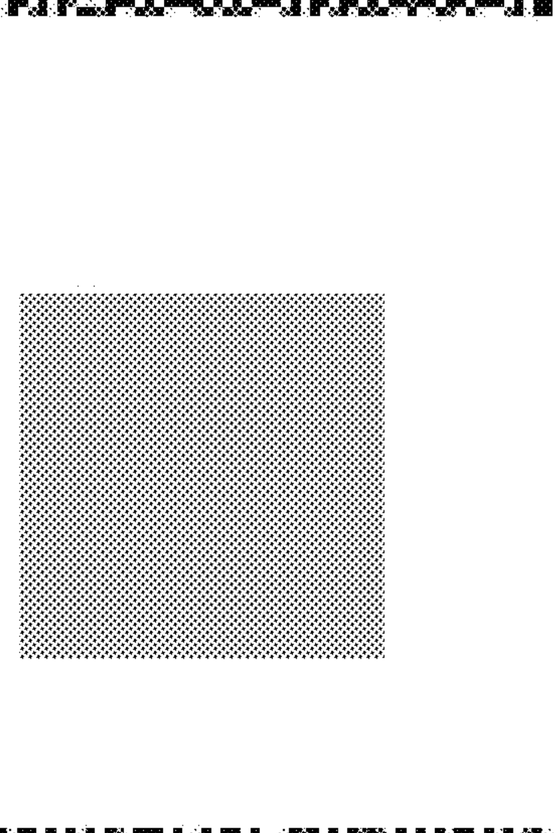

Barycentric Error Diffusion

R,G,B = 188, 170, 149

Figure 10

METHOD AND APPARATUS FOR RENDERING COLOR IMAGES

REFERENCE TO RELATED APPLICATIONS

This application is related to and claims priority to U.S. Provisional Application 63/108,855 filed on Nov. 2, 2020.

The entire disclosures of the aforementioned application is herein incorporated by reference.

SUBJECT OF THE INVENTION

This invention relates to methods for driving electro-optic displays. More specifically, this invention relates to driving methods for dithering and rendering images on electrophoretic displays.

BACKGROUND

This invention relates to a method and apparatus for rendering color images. More specifically, this invention relates to a method for multi-color dithering, where a combination of color intensities are converted into a multi-color surface coverage.

The term "pixel" is used herein in its conventional meaning in the display art to mean the smallest unit of a display capable of generating all the colors which the display itself can show.

Half-toning has been used for many decades in the printing industry to represent gray tones by covering a varying proportion of each pixel of white paper with black ink. Similar half-toning schemes can be used with CMY or CMYK color printing systems, with the color channels being varied independently of each other.

However, there are many color systems in which the color channels cannot be varied independently of one another, in as much as each pixel can display any one of a limited set of primary colors (such systems may hereinafter be referred to as "limited palette displays" or "LPD's"); the ECD patent color displays are of this type. To create other colors, the primaries must be spatially dithered to produce the correct color sensation.

Electronic displays typically include an active matrix backplane, a master controller, local memory and a set of communication and interface ports. The master controller receives data via the communication/interface ports or retrieves it from the device memory. Once the data is in the master controller, it is translated into a set of instruction for the active matrix backplane. The active matrix backplane receives these instructions from the master controller and produces the image. In the case of a color device, on-device gamut computations may require a master controller with increased computational power. As indicated above, rendering methods for color electrophoretic displays are often computational intense, and although, as discussed in detail below, the present invention itself provides methods for reducing the computational load imposed by rendering, both the rendering (dithering) step and other steps of the overall rendering process may still impose major loads on device computational processing systems.

The increased computational power required for image rendering diminishes the advantages of electrophoretic displays in some applications. In particular, the cost of manufacturing the device increases, as does the device power consumption, when the master controller is configured to perform complicated rendering algorithms. Furthermore, the extra heat generated by the controller requires thermal management. Accordingly, at least in some cases, as for example when very high resolution images, or a large number of images need to be rendered in a short time, it may be desirable to have an efficient method for dithering multi-colored images.

SUMMARY OF INVENTION

Accordingly, in one aspect, the subject matter presented herein provides for a method for driving an electro-optic display, the method can include receiving an input image, processing the input image to create color separation cumulate, and dithering the input image by intersecting the color separation cumulate with a dither function.

In some embodiments, the dither function is a threshold array.

In another embodiment, the threshold array is a Blue Noise Mask (BNM).

In yet another embodiment, the step of processing is implemented by a look up table.

BRIEF DESCRIPTION OF DRAWINGS

The patent or application file contains at least one drawing executed in color. Copies of this patent or patent application publication with color drawing(s) will be provided by the Office upon request and payment of the necessary fee.

FIG. **1** of the accompanying drawings is an image rendering model in accordance with the subject matter presented herein;

FIG. **2** is an exemplary black and white dithering method using masks in accordance with the subject matter presented herein;

FIG. **3** illustrates various mask designs in accordance with the subject matter presented herein;

FIG. **4** illustrates a gamut color mapping in accordance with the subject matter disclosed herein;

FIG. **5** illustrates a multi-color dithering method using masks in accordance with the subject matter disclosed herein;

FIG. **6** illustrates a multi-color dithering algorithm using masks in accordance with the subject matter disclosed herein; and

FIGS. **7-10** are various mask designs for multi-color dithering in accordance with the subject matter presented herein.

DETAILED DESCRIPTION

Standard dithering algorithms such as error diffusion algorithms (in which the "error" introduced by printing one pixel in a particular color which differs from the color theoretically required at that pixel is distributed among neighboring pixels so that overall the correct color sensation is produced) can be employed with limited palette displays. There is an enormous literature on error diffusion; for a review see Pappas, Thrasyvoulos N. "Model-based halftoning of color images," IEEE Transactions on Image Processing 6.7 (1997): 1014-1024.

This application is also related to U.S. Pat. Nos. 5,930,026; 6,445,489; 6,504,524; 6,512,354; 6,531,997; 6,753,999; 6,825,970; 6,900,851; 6,995,550; 7,012,600; 7,023,420; 7,034,783; 7,061,166; 7,061,662; 7,116,466; 7,119,772; 7,177,066; 7,193,625; 7,202,847; 7,242,514; 7,259,744; 7,304,787; 7,312,794; 7,327,511; 7,408,699; 7,453,445; 7,492,339; 7,528,822; 7,545,358; 7,583,251; 7,602,374; 7,612,760; 7,679,599; 7,679,813; 7,683,606; 7,688,

297; 7,729,039; 7,733,311; 7,733,335; 7,787,169; 7,859,742; 7,952,557; 7,956,841; 7,982,479; 7,999,787; 8,077,141; 8,125,501; 8,139,050; 8,174,490; 8,243,013; 8,274,472; 8,289,250; 8,300,006; 8,305,341; 8,314,784; 8,373,649; 8,384,658; 8,456,414; 8,462,102; 8,514,168; 8,537,105; 8,558,783; 8,558,785; 8,558,786; 8,558,855; 8,576,164; 8,576,259; 8,593,396; 8,605,032; 8,643,595; 8,665,206; 8,681,191; 8,730,153; 8,810,525; 8,928,562; 8,928,641; 8,976,444; 9,013,394; 9,019,197; 9,019,198; 9,019,318; 9,082,352; 9,171,508; 9,218,773; 9,224,338; 9,224,342; 9,224,344; 9,230,492; 9,251,736; 9,262,973; 9,269,311; 9,299,294; 9,373,289; 9,390,066; 9,390,661; and 9,412,314; and U.S. Patent Applications Publication Nos. 2003/0102858; 2004/0246562; 2005/0253777; 2007/0091418; 2007/0103427; 2007/0176912; 2008/0024429; 2008/0024482; 2008/0136774; 2008/0291129; 2008/0303780; 2009/0174651; 2009/0195568; 2009/0322721; 2010/0194733; 2010/0194789; 2010/0220121; 2010/0265561; 2010/0283804; 2011/0063314; 2011/0175875; 2011/0193840; 2011/0193841; 2011/0199671; 2011/0221740; 2012/0001957; 2012/0098740; 2013/0063333; 2013/0194250; 2013/0249782; 2013/0321278; 2014/0009817; 2014/0085355; 2014/0204012; 2014/0218277; 2014/0240210; 2014/0240373; 2014/0253425; 2014/0292830; 2014/0293398; 2014/0333685; 2014/0340734; 2015/0070744; 2015/0097877; 2015/0109283; 2015/0213749; 2015/0213765; 2015/0221257; 2015/0262255; 2015/0262551; 2016/0071465; 2016/0078820; 2016/0093253; 2016/0140910; and 2016/0180777. These patents and applications may hereinafter for convenience collectively be referred to as the "MEDEOD" (MEthods for Driving Electro-Optic Displays) applications, and are incorporated herein in their entirety by reference.

ECD systems exhibit certain peculiarities that must be taken into account in designing dithering algorithms for use in such systems. Inter-pixel artifacts are a common feature in such systems. One type of artifact is caused by so-called "blooming"; in both monochrome and color systems, there is a tendency for the electric field generated by a pixel electrode to affect an area of the electro-optic medium wider than that of the pixel electrode itself so that, in effect, one pixel's optical state spreads out into parts of the areas of adjacent pixels. Another kind of crosstalk is experienced when driving adjacent pixels brings about a final optical state, in the area between the pixels that differs from that reached by either of the pixels themselves, this final optical state being caused by the averaged electric field experienced in the inter-pixel region. Similar effects are experienced in monochrome systems, but since such systems are one-dimensional in color space, the inter-pixel region usually displays a gray state intermediate the states of the two adjacent pixel, and such an intermediate gray state does not greatly affect the average reflectance of the region, or it can easily be modeled as an effective blooming. However, in a color display, the inter-pixel region can display colors not present in either adjacent pixel.

The aforementioned problems in color displays have serious consequences for the color gamut and the linearity of the color predicted by spatially dithering primaries. Consider using a spatially dithered pattern of saturated Red and Yellow from the primary palette of an ECD display to attempt to create a desired orange color. Without crosstalk, the combination required to create the orange color can be predicted perfectly in the far field by using linear additive color mixing laws. Since Red and Yellow are on the color gamut boundary, this predicted orange color should also be on the gamut boundary. However, if the aforementioned effects produce (say) a blueish band in the inter-pixel region between adjacent Red and Yellow pixels, the resulting color will be much more neutral than the predicted orange color. This results in a "dent" in the gamut boundary, or, to be more accurate since the boundary is actually three-dimensional, a scallop. Thus, not only does a naïve dithering approach fail to accurately predict the required dithering, but it may as in this case attempt to produce a color which is not available since it is outside the achievable color gamut.

It may desirable for one to be able to predict the achievable gamut by extensive measurement of patterns or advanced modeling. This may be not be feasible if the number of device primaries is large, or if the crosstalk errors are large compared to the errors introduced by quantizing pixels to a primary colors. The present invention provides a dithering method that incorporates a model of blooming/crosstalk errors such that the realized color on the display is closer to the predicted color. Furthermore, the method stabilizes the error diffusion in the case that the desired color falls outside the realizable gamut, since normally error diffusion will produce unbounded errors when dithering to colors outside the convex hull of the primaries.

In some embodiments the reproduction of images may be performed using an Error-Diffusion model illustrated in FIG. **1** of the accompanying drawings. The method illustrated in FIG. **1** begins at an input **102**, where color values $x_{i,j}$ are fed to a processor **104**, where they are added to the output of an error filter **106** to produce a modified input $u_{i,j}$, which may hereinafter be referred to as "error-modified input colors" or "EMIC". The modified inputs $u_{i,j}$ are fed to a Quantizer **108**.

In some embodiments, processes utilizing model-based error diffusion can become unstable, because the input image is assumed to lie in the (theoretical) convex hull of the primaries (i.e. the color gamut), but the actual realizable gamut is likely smaller due to loss of gamut because of dot overlap. Therefore, the error diffusion algorithm may be trying to achieve colors which cannot actually be achieved in practice and the error continues to grow with each successive "correction". It has been suggested that this problem be contained by clipping or otherwise limiting the error, but this leads to other errors.

In practice, one solution would be to have a better, non-convex estimate of the achievable gamut when performing gamut mapping of the source image, so that the error diffusion algorithm can always achieve its target color. It may be possible to approximate this from the model itself, or determine it empirically. In some embodiments, the quantizer **108** examines the primaries for the effect that choosing each would have on the error, and the quantizer chooses the primary with the least (by some metric) error if chosen. However, the primaries fed to the quantizer **108** are not the natural primaries of the system, $\{P_k\}$, but are an adjusted set of primaries, $\{\tilde{P}_k\}$, which allow for the colors of at least some neighboring pixels, and their effect on the pixel being quantized by virtue of blooming or other inter-pixel interactions.

One embodiment of the above method may use a standard Floyd-Steinberg error filter and processes pixels in raster order. Assuming, as is conventional, that the display is treated top-to-bottom and left-to-right, it is logical to use the above and left cardinal neighbors of pixel being considered to compute blooming or other inter-pixel effects, since these two neighboring pixels have already been determined. In this way, all modeled errors caused by adjacent pixels are accounted for since the right and below neighbor crosstalk is accounted for when those neighbors are visited. If the model only considers the above and left neighbors, the

adjusted set of primaries must be a function of the states of those neighbors and the primary under consideration. The simplest approach is to assume that the blooming model is additive, i.e. that the color shift due to the left neighbor and the color shift due to the above neighbor are independent and additive. In this case, there are only "N choose 2" (equal to N*(N−1)/2) model parameters (color shifts) that need to be determined. For N=64 or less, these can be estimated from colorimetric measurements of checkerboard patterns of all these possible primary pairs by subtracting the ideal mixing law value from the measurement.

To take a specific example, consider the case of a display having 32 primaries. If only the above and left neighbors are considered, for 32 primaries there are 496 possible adjacent sets of primaries for a given pixel. Since the model is linear, only these 496 color shifts need to be stored since the additive effect of both neighbors can be produced during run time without much overhead. So for example if the unadjusted primary set comprises (P**1** . . . P**32**) and your current up, left neighbors are P**4** and P**7**, the modified primaries ($\tilde{P}_1 \ldots \tilde{P}_{32}$), the adjusted primaries fed to the quantizer are given by:

$$\tilde{P}_1 = P_1 + dP_{(1,4)} + dP_{(1,7)};$$

.....

$$\tilde{P}_{32} = P_{32} + dP_{(32,4)} + dP_{(32,7)},$$

where $dP_{(i,j)}$ are the empirically determined values in the color shift table.

More complicated inter-pixel interaction models are of course possible, for example nonlinear models, models taking account of corner (diagonal) neighbor, or models using a non-causal neighborhood for which the color shift at each pixel is updated as more of its neighbors are known.

The quantizer **108** compares the adjusted inputs $u'_{i,j}$ with the adjusted primaries $\{\tilde{P}_k\}$ and outputs the most appropriate primary $y_{i,k}$ to an output. Any appropriate method of selecting the appropriate primary may be used, for example a minimum Euclidean distance quantizer in a linear RGB space; this has the advantage of requiring less computing power than some alternative methods.

The $y_{i,k}$ output values from the quantizer **108** may be fed not only to the output but also to a neighborhood buffer **110**, where they are stored for use in generating adjusted primaries for later-processed pixels. The modified input $u_{i,j}$ values and the output $y_{i,j}$ values are both supplied to a processor **112**, which calculates:

$$e_{i,j}=u_{i,j}-y_{i,j}$$

and passes this error signal on to the error filter **106** in the same way as described above with reference to FIG. **1**.

However, in practice, error diffusion based methods may be slow for some applications because they are not easily parallelizable. Where the next pixel output cannot be completed until a previous pixel's output becomes available. Alternatively, masked based methods may be adopted because of their simplicity, where the output at each pixel depends only on that pixel's input and a value from a look-up-table (LUT), meaning, each output can be computed completely independently of others.

Referring now to FIG. **2**, where an exemplary black and white dithering method is illustrated. As shown, an input grayscale image with normalized darkness values between 0 (white) and 1 (black) is dithered by comparing at each output location corresponding input darkness and dither threshold values. For example, if the darkness u(x) of an input image is higher than the dither threshold value T(x), then the output location is marked as black (i.e., 1), else it is marked as white (i.e., 0). FIG. **3** illustrates some mask designs in accordance with the subject matter disclosed herein.

In practice, when practicing multi-color dithering, it is assumed that the input colors to a dithering algorithm can be represented as a linear combination of multi-primaries. This may be achieved by dithering in the source space using gamut corners, or by gamut mapping the input to the device space color gamut. FIG. **4** illustrates one method of creating a color separation using a set of weights Px. Where each color C is defined as—

$$C = \sum_{i=1,\ldots N} \alpha_i(C)P_i \quad 0 \le \alpha_i \le 1, \sum \alpha_i = 1$$

Where the partial sums of these weights is referred to as separation cumulate $\Lambda_k(C)$, where

$$\Lambda_k(C) = \sum_{i=1,\ldots k} \alpha_i(C)$$

In practice, dithering to multiple colors consists in intersecting the relative cumulative amounts of colors with a dither function (e.g., threshold array T(x) **502** of FIG. **5**). Referring now to FIG. **5**, illustrated here as an example is a method to print with **4** different colors inks C_1 **512**, C_2 **514**, C_3 **516** and C_4 **518**. At each pixel of the output pixmap, the color separation gives the relative percentages of each of the basic colors, for example d_1 of color C_1 **512**, d_2 of color C_2 **514**, d_3 of color C_3 **516**, and d_4 of color C_4 **518**. Where one of the colors, for example C_4 **518**, may be white.

Extending dithering to multiple colors consists in intersecting the relative cumulative amounts of colors $\Lambda_1(x)$ **504**=d1, $\Lambda_2(x)$ **506**=d1+d2, $\Lambda_3(x)$ **508**=d1+d2+d3, and $\Lambda_4(x)$ **510**=d1+d2+d3+d4 with a threshold array T(x), as illustrated in FIG. **5**. Illustrated in FIG. **5** is a dithering example for the purpose of explaining the subject matter presented herein. In the interval where $\Lambda_1(x)$ **504**>T(x) **502**, the output location or pixel region will be printed with basic color C_1 **512** (e.g., black); in the interval where $\Lambda_2(x)$ **506**>T(x) **502**, the output location or pixel region will display color C_2 **514** (e.g., yellow); in the interval where $\Lambda_3(x)$ **508**>T(x) **502**, the output location or pixel region will display color C_3 **516** (e.g., red); and in the remaining interval where $\Lambda_4(x)$ **510**>T(x) **502** and $\Lambda_3(x)$ **508**≤T(x) **502**, the output location or pixel region will display color C_4 **518** (e.g., white). As such, multi-color dithering as presented herein will convert the relative amounts of d_1, d_2, d_3, d_4 of colors C_1 **512**, C_2 **514**, C_3 **516** and C_4 **518** into relative coverage percentages and ensures by construction that the contributing colors are printed side by side.

In some embodiments, a multi-color rendering algorithm as illustrated in FIG. **6** may be utilized in accordance with the subject matter disclosed herein. As shown, image data $im_{i,j}$ may be firstly fed through a sharpening filter **602**, which may be optional in some embodiments. This sharpening filter **602** may be useful in some cases when a threshold array T(x) or filter is less sharp than an error diffusion system. This sharpening filter **602** may be a simple finite impulse response (FIR) filter, for example 3×3, which may

be easily computed. Subsequently, color data may be mapped in a color mapping step **604**, and color separation may be generated in a separation generation step **606** by methods commonly available in the art, such as using the Barycentric coordinate method, and this color data may be used to index a CSC_LUT look up table, which can have N-entries per index that gives the desired separation information in the form that is directly needed by the mask based dithering step (e.g., step **612**). In some embodiments, this CSC_LUT look up table may be built by combining both a desired color enhancement and/or gamut mapping, and the chosen separation algorithm, and is configured to include a mapping between the input image's color values and the color separation cumulate. In this fashion, the look up table (e.g., CSC_LUT) may be designed to provide the desired separation cumulate information quickly and in the form that is directly needed by the mask based dithering step (e.g., step **612** with the quantizer). Finally, the separation cumulate data **608** is used with a threshold array **610** to generate an output $y_{i,j}$ using a quantizer **612** to generate multiple colors. In some embodiments, the color mapping **604**, separation generation **606** and cumulate **608** step may be implemented as a single interpolated CSC_LUT look up table. In this configuration, the separation stage is not done by finding Barycentric coordinates in a tetrahedralization of the multi-primaries, but may be implemented by a look-up table, which allows more flexibility. In addition, output computed by the method illustrated herein is computed completely independently of the other outputs. Furthermore, the threshold array T(x) used herein may be a Blue Noise Mask (BNM), where various BNM designs are presented in FIG. **7-10**.

It will be apparent to those skilled in the art that numerous changes and modifications can be made in the specific embodiments of the invention described above without departing from the scope of the invention. Accordingly, the whole of the foregoing description is to be interpreted in an illustrative and not in a limitative sense.

The invention claimed is:

1. A method for driving an electro-optic display having a plurality of display pixels, the method comprising:

receiving an input image;

processing the input image to create color separation cumulate; and

dithering the input image by intersecting the color separation cumulate with a dither function.

2. The method of claim **1** wherein the dither function is a threshold array.

3. The method of claim **2** wherein the threshold array is a Blue Noise Mask (BNM).

4. The method of claim **3** wherein the look up table includes a mapping between the input image's color values and the color separation cumulate.

5. The method of claim **4** wherein the sharpening filter is a finite impulse response (FIR) filter.

6. The method of claim **1** wherein the processing the input image step is implemented by a look up table.

7. The method of claim **1** further comprising putting the input image through a sharpening filter before processing the input image.

8. The method of claim **1**, wherein the step of processing the input image to create color separation cumulate includes using a Barycentric coordinate method.

9. An electro-optic display configured to carry out the method of claim **1** includes an electrophoretic display.

10. The display according to claim **9** comprising rotating bichromal member, electrochromic or electro-wetting material.

11. The electro-optic display according to claim **9** comprising an electrophoretic material comprising a plurality of electrically charged particles disposed in a fluid and capable of moving through the fluid under the influence of an electric field.

12. The electro-optic display according to claim **11** wherein the electrically charged particles and the fluid are confined within a plurality of capsules or microcells.

13. The electro-optic display according to claim **11** wherein the electrically charged particles and the fluid are present as a plurality of discrete droplets surrounded by a continuous phase comprising a polymeric material.

* * * * *